Magnetic Field Quality Investigations for Superconducting Super Collider Magnets

by

Richard F. Gunst and William R. Schucany
Department of Statistical Science
Southern Methodist University
Dallas, Texas 75275

Technical Report No. SMU/DS/TR-282

Magnetic Field Quality Investigations for Superconducting Super Collider Magnets

Richard F. Gunst and William R. Schucany

Department of Statistical Science

Southern Methodist University

Dallas, Texas 75275-0332

Table of Contents

I. Introduction

II. Magnetic Field Quality

III. Statistical Control

- A .Multipole Variability
- B. Conformance to Specification
- C. Azimuthal Coil-Size Measurements
- D. Azimuthal Coil-Size Measurements in Diagonally Opposite Quadrants

IV. Predicting Magnet Field Quality

- A. Spatial Correlations
  - A.1 Spatial Autocorrelations
  - A.2 Spatial Semivariograms
- B. Azimuthal Coil-Size Measurements
- C. Cold/Warm Measurements

V. Concluding Remarks

Abstract

This article describes initial quality assurance efforts for certifying the satisfactory performance of large dipole magnets that were to be major components of the Superconducting Super Collider. Many physical characteristics of the magnets and their construction, as well as the measurement of magnetic field quality, posed unique challenges for these quality assurance efforts, not the least of which was the need to use indirect measurements of the magnetic field. In this article, the statistical issues that were addressed prior to the cancellation of the project are described. Several of these investigations suggest promising indications of satisfactory magnet performance based on novel applications of a variety of statistical process control and modeling methods. The challenge of successfully implementing the requisite monitoring and certification methods that were being devised for the full-scale production process ceased with the cancellation of the project. Nevertheless, the lessons learned from these investigations benefit ongoing quality assurance efforts at other sites where scientific research using large particle accelerators continues.

I. Introduction

The demise of the Superconducting Super Collider (SSC) project ended a unique opportunity for the development and implementation of novel quality assurance methods on a scientific program of immense potential and importance. The SSC was to have consisted of two 54 mile rings of approximately 12,000 powerful magnets that were to accelerate and turn beams of protons in opposite directions until the two beams collided with forces unavailable in any other particle beam accelerator in existence. In addition to its importance for the study of the basic building blocks of nature, construction of the SSC posed immense technological challenges. The SSC specifications required magnets that would accelerate protons to 3,400 revolutions per second around the collider rings, properly focus proton beams that were a few millimeters in diameter, and ultimately allow

the protons to collide. Among the many scientific challenges was the study of novel statistical procedures needed to ensure that the individual magnets met the specifications required for proper functioning. Since the installment of the magnets was to take place over a minimum of four years, quality assurance methods needed to be able to predict individual magnet performance with a high degree of certitude long before current would actually flow through the completed collider ring. The experiments in particle physics initially were scheduled to begin in 1999.

Due to the close proximity of the Supercollider site and Southern Methodist University, members of its Physics Department were involved with the project from the outset. Some newer members of that department were recruited and hired because of the potential for interaction with other particle physicists on unique experiments involving the Supercollider. Early on in the planning stages, it also became apparent that statstical expertise would be needed both in the design and analysis of some of the experiments and, of more immediate importance, in establishing a quality assurance program for mangnet acceptance. Members of the Department of Statistical Science were then recruited to participate in these activities.

Approximately 8,000 of the magnets in the Super Collider were to be dipole turning magnets. Additional magnets were to be constructed in smaller numbers for focusing and accelerating the proton beam. Each of the dipole magnets was to be approximately 15 meters in length. These magnets were to be delivered by manufacturers at a rate of about four per day and were to be installed at the same rate in the collider ring tunnel. Since only a small storage facility was planned, this delivery and installation rate placed a great demand on quality assurance methods for magnet acceptance. In order to meet budget requirements, it was hoped that magnet performance could be satisfactorily assessed without extensive testing of each magnet on delivery. Furthermore, if individual magnet testing was needed, it was much more economical to test magnets under warm (room temperature) environmental conditions, not the cryogenic (near absolute zero, 4°

Kelvin) conditions that were to be the normal operating conditions of the SSC for optimal magnet performance.

The ultimate development of the necessary quality assurance methods was not completed due to the cancellation of the project in 1993. Nevertheless, a number of quality assurance issues were addressed and progress was made in their resolution. Statisticians involved with the project brought uniques skills to the team of particle physicists, magnet scientists, and manufacturing engineers. The tools of modern data analysis, computer graphics, and statistical models for dependence structures provided novel dimensions to the initial scientific investigations. This paper reports on some of the initial investigations. Section II describes the unique measurements that constituted the key measures of magnet quality. One of the unique facets of the investigation is that magnet field quality was not directly measured. Rather magnet field quality was to be assessed by the magnitudes of individual Fourier coefficients fitted to measured series of voltages. In Section III, preliminary studies of the stability of the multipole coefficients are reported. Lack of statistical control in the calculated coefficients of prototype magnets were identified using traditional plotting methods. Section IV discusses the feasibility of using physical measurements of the magnets instead of, or in addition to, the magnetic field measurements of the multipole coefficients. Both coil size measurements and warm multipole measurements were found to be promising as predictors of cryogenic magnet performance. Concluding remarks are made in Section V.

II. Magnetic Field Quality

Magnetic fields in dipole magnets are produced by running strong electrical currents through oval windings of conducting wire coils along the top and the bottom of the cylindrical housing of the cryogenic components of the magnets. This is depicted in the schematic cross-section shown in Figure 1. A proton passing through an induced vertical magnetic field ideally would be deflected horizontally to the right or to the left depending

on the direction of the current flow. Departures from a perfect vertical field affect magnet performance because the protons are not deflected solely in the horizontal direction. Field imperfections can be caused by any of a large number of problems. Of special importance to quality assurance were a variety of possible imperfections in the magnet construction. For example, the coils must be held in place by steel collars that are formed from hundreds of laminations of thin plates. Imperfections in the laminations themselves or in the processes of pressing the laminations on to the coil windings could degrade magnet performance.

Magnetic field fluxes can be directly measured from voltage differences across the field. For technical reasons, the voltages themselves are not the quantities of interest in gauging the field quality of SSC magnets. Instead, the key quality measurements are the calculated coefficients in a Fourier series representation of the field. The magnetic field harmonics for SSC magnets are given by

$$B_y + iB_x = B_0 \sum_{k=0}^{\infty} \{b_k + ia_k\}\{\cos(k\theta) + i\sin(k\theta)\}(r/R)^k ,$$

where B_y and B_x are, respectively, the vertical and horizontal components of the field at a point whose polar coordinates from the center of the beam aperture are (r,θ), and B_0 is the magnitude of the field at midplane at the maximum nominal radius R = 10 mm. The coefficients b_k and a_k are referred to as the normal and the skew *multipole coefficients*, respectively. For a magnet with perfect dipole symmetry, only the even normal multipoles b_{2k} are nonzero. These are referred to as the "allowed" multipoles for SSC magnets. Thus, the quality of the magnetic field is determined by whether a magnet's multipole coefficients were sufficiently close to prescribed values. Although the multipole coefficients are calculated values from voltages, they will be referred to as multipole measurements in this article.

Magnet scientists developed these theoretical models and experimented with actual construction and measurement methodology on particle accelerators elsewhere in the

world. Much of the physics and engineering was well documented and understood. However, the size of the SSC was pushing the frontiers of material properties and manufacturing capabilities.

III. Statistical Control

Magnetic field theory and extensive computer simulations led physicists to prescribe the limits shown in Table 1 for the first four allowed and unallowed multipole coefficients. Variability in multipole coefficients comes from numerous sources. In general, it is recognized that there are (a) nonuniformities in the materials that are used to make magnets and (b) inaccuracies throughout the manufacturing process. Prior to initial investigations of the actual sources of multipole variation, it was decided to evaluate the magnitude of the combined effects of these disturbances, both within (along the 15 meter length of a magnet) and between magnets. Furthermore, to derive guidelines for identifying unacceptable magnets, estimates of the standard deviations of coefficients obtained from different magnets were needed.

Numerous measurement were taken on nine prototype dipole magnets, labeled DCA311-DCA319. Due to the physical size of the device (referred to as a "mole") used to measure voltages, magnetic field data were collected at positions every 0.6 meters along the lengths of the magnets. In addition, a number of physical measurements of the coils and other components of the magnets were made in addition to measurements of the field quality; i.e., the multipole coefficients. On some of the magnets, multipole coefficients were obtained under both warm and cold temperatures. Cold measurements were taken on all nine prototype magnets. All of these measurements contributed to the understanding of magnetic field variation across magnets, as well as to variations in the measurement process.

Principal component analyses of vectors of multipole coefficients for the prototype magnets resulted in individual multipole values receiving almost all the weight in each

component. This analysis and others did not lead to any substantive evidence that the multipole coefficient values for a single magnet were correlated. Hence, individual multipoles coefficients were analyzed separately. Some of the analyses that were conducted are described in the following sections.

A. Multipole Variability

Figure 2 is a representative plot for repeat measurements on skew multipole a_1 for two magnets, DCA311 and DCA314. The four repeat measurements are plotted by position along the length of the magnet, axis z in Figure 1. The positions are in meters from the center of each magnet. The repeat measurements are virtually identical on the scale plotted in Figure 2. There clearly is much greater variability associated with the positions along the magnet and between the two magnets than there is among the four repeats. These features of Figure 2 suggest, as was confirmed by formal analyses, that the repeat measurement error was very small relative to variability from other sources.

The effects on the value of a_1, for example, due to magnets and positions can be assessed using a random effects analysis of variance model:

$$y_{ijk} = \mu + m_i + p_j + (mp)_{ij} + e_{ijk} \ ,$$

where y_{ijk} is the a_1 multipole value for the ith magnet (i = 1, ... , M), the jth position (j = 1, ... , P), and the kth repeat (k = 1, ... , K). The terms in the model are an overall constant mean effect μ, random main effects m_i for the magnets, p_j for positions, and $(mp)_{ij}$ for their random interactions. The constant term μ is nominally the target magnitude for the multipole. This specification value, 0.04, is shown in Table 1. Satisfactory magnet performance requires that the a_1 multipole achieve this target within close limits. Using the rms specification limit (1.25) shown in the table as a reasonable limit of variability, the plotted multipole coefficients in Figure 2 suggest that these two magnets do achieve the desired mean value within acceptable control limits.

The effects of position and magnet are modeled as random effects because they would not be expected to be systematically similar on each dipole magnet. The random effects are treated as independent normal variates with zero means and variances σ_m^2, σ_p^2, and σ_{mp}^2. The random measurement errors are modeled similarly, with the measurement error variance denoted by σ_e^2.

An analysis was performed on six prototype SSC dipole magnets, identified as magnets DCA311, DCA314, and DCA316-319. Twenty-four fixed positions on the magnet were used; the two end positions were not included because of known "edge effects" which had to be treated differently. Table 2 is the analysis of variance table for these data. The measurement error standard deviation estimate is consistent with the anticipated variation of 0.01. Note the larger estimated variance for the magnet effects and the magnet by position interaction. This analysis indicates that the largest effects in these prototype magnets was indeed magnet-to-magnet differences. From the estimates in Table 2 one can calculate an estimate of the variability expected for a single magnet, averaging across positions and repeats. This standard deviation estimate $\hat{\sigma}_M$ is

$$\begin{aligned}\hat{\sigma}_M &= \{\hat{\sigma}_m^2 + P^{-1}(\hat{\sigma}_p^2 + \hat{\sigma}_{mp}^2) + P^{-1}K^{-1}\hat{\sigma}_e^2\}^{1/2} \\ &= 0.391 .\end{aligned}$$

This is a very small increase from the estimated standard deviation of the magnet main effect, $\hat{\sigma}_m = 0.387$, and is well within the rms specification in Table 1, suggesting from this very limited analysis that the magnet-to-magnet variation in a_1 skew multipoles would be capable of achieving the desired specifications for acceptable magnet performance.

All analyses of the allowed and unallowed multipole coefficients indicated that the magnet main effect was the dominant effect when multipole values were averaged across positions. Since the anticipated quality assurance procedures were to utilize multipole coefficients averaged across positions, this finding was important.

Some technical issues remain concerning the validity of this analysis. One is the concern that the measurements at adjacent positions might be spatially correlated. In the above model, correlations do exist in measurements at different positions through the random effects for position and for magnet by position interaction, but these correlations are constant for any pair of positions. Spatial analyses that permit decreasing correlations as a function of the increasing distance between positions are investigated in Section IV.

B. Conformance to Specification

A comprehensive analysis of the conformance to the magnetic field specifications could not be performed with data from only six to nine prototype magnets. As additional prototype magnets were built and in the early stages of production, more extensive investigations were planned to assure that quality control methods derived during the development phase of the project were indeed suitable for an assessment of magnet performance. Nevertheless, it was of considerable interest to obtain some sense from the prototype magnets about the conformance to the design specifications for the multipole values. From analyses similar to those performed in the last section, estimated magnet standard deviations for the first few -- the only truly important -- multipoles were obtained. Ratios of these estimated standard deviations to the specified rms values in Table 1 are plotted in Figure 3 for the first six normal and skew multipoles. All the ratios are well below 1.0, in the range of 0.10 to 0.56, indicating good conformance to specification.

C. Azimuthal Coil-Size Measurements

The magnetic field in SSC dipole magnets is induced by current flowing in opposite directions through two sets of coil windings, one set on the top of the magnet and one on the bottom. At cryogenic conditions, more than 6,000 amps of current were to

flow through these coils. Imperfections in the coils or any lack of symmetry in their geometric positioning could lead to distortions of the magnetic field.

Prototype coils were wound separately around the length of the top and the bottom halves of the beam tube. For each half, two sets of coils, labeled the *inner* and the *outer* coils, were needed to produce the correct vertical magnetic field. They were pressed into place with laminated *collars* using hydraulic presses under high temperatures until they were cured. When viewed from the front of a vertical slice through the magnet, the coil windings looked somewhat like the schematic in Figure 1. After curing and prior to the binding of each half of the magnet together to form the complete magnet configuration, physical coil-size measurements could easily be taken at each position along the magnet halves. Interest in the azimuthal size measurements (inner, outer, left, and right) focused on two characteristics. First, any systematic variation along the length of the coils would suggest a problem with the manufacture of coil or collar laminations or with the pressing or curing processes. Second, if random variation in the coil sizes could be related to magnetic field quality, then these easily taken measurements could be used in the quality control procedures.

Figure 4 is an illustrative graph of the deviations of azimuthal coil-size measurements from a master coil. These deviation measurements were taken on prototype magnets DCA311-319 for the inner coils located in the lower left quadrant of the respective magnets. A total of 192 coil-size measurements are displayed for each coil. The measurements were taken at the centers of three inch segments along the length of the magnets. The deviations are plotted versus the position from the center line of the coil windings to the centers of the three-inch segments. The measurements plotted in Figure 4 convey very striking systematic patterns. Of particular note are the three downward spikes, one at the first measurement location to the left of the center line and two more at approximately 170-180 inches to the left and to the right of the center line. Other more cyclic patterns are also discernible. These general patterns appeared in plots of all the inner

and the outer coils for all nine prototype magnets. It was conjectured that the three precipitous downward spikes might be due to the locations of the three pistons that exerted pressure on the curing bars used to press the coils onto the beam tubes. It is not known whether engineers investigated or found a reason for the apparent cyclical patterns in the coil size measurements.

D. Azimuthal Coil-Size Measurements in Diagonally Opposite Quadrants

Another factor in the geometry of the coils is asymmetry in the placement of opposite quadrant coils. Magnets having top-bottom asymmetry in the placement of coils would have nonzero odd skew multipoles a_{2n-1} in addition to the allowed even normal multipoles b_{2n}. Magnets having left-right asymmetry would have nonzero odd normal multipoles b_{2n-1} in addition to the allowed even multipoles. Other types of asymmetry could produce a wide variety of nonzero nonallowed multipoles. One primary concern of the magnet scientists was the symmetry of the coil halves in diagonally opposite quadrants of the assembled magnet.

Figure 5 presents a comparison of opposite diagonal quadrant coil-size measurements for coils 1012 (upper right quadrant, Quadrant I) and 1013 (lower left quadrant, Quadrant III) for magnet DCA314. There is a clear shift in the coil-size measurements evident in the upper left panel in Figure 5, with the (dashed) Quadrant III measurements larger than those for the (solid) Quadrant I measurements. Although there is a good correlation between the two sets of measurements indicated in the upper right panel of the figure, the average of the two sets of measurements shown in the lower left panel exhibits a quadratic-like trend across the length of the magnet. Finally, the differences in the coil-size measurements shown in the lower right panel not only indicate a clear negative bias, but they also suggest a distinct cyclic pattern across the length of the magnet.

These findings suggest that there were asymmetries in the coil size measurements that might have an effect on magnet performance. The combination of coil-size measurements and other physical measurements ultimately were to be used to determine whether magnet performance could be satisfactorily assessed, perhaps along with warm (10 amps, room temperature) magnetic field measurements. Initial investigations of the ability to predict cold (6,000 amps, $4^{o}K$) magnet performance from physical magnet characteristics and warm multipole values had just been initiated when the SSC project was terminated. These preliminary investigations not only suggested that this goal could be achieved, they also posed some interesting statistical challenges. Some of these initial findings are now summarized.

IV. Predicting Magnet Field Quality

A primary goal for magnet acceptance quality control methods was to certify magnets based on physical measurements of the coils and other magnet components and on room-temperature ("warm") magnetic field measurements. It was also desired that magnet acceptance be based on average magnet measurements and not on individual measurements taken along the length of the magnet. For example, average coil-size measurements were to be used rather than the individual 192 coil-size measurements taken along the length of the coil. While investigations of these issues was far from complete, some preliminary studies that were important to the resolution of these issues were undertaken. The results are reported in this section. These investigations focused on (a) the critically important assumption of the spatial independence of coil-size measurements, (b) the potential for adequate prediction of magnet multipoles from coil-size measurements, and (c) the potential for adequate prediction of cryogenic magnet performance from test results taken under room temperatures.

A. Spatial Correlations

Measurements along the length of a fifteen-meter magnet could very easily be spatially correlated. While this would not affect the use of an average as an overall measure of magnet performance, the ordinary average is not efficient when observations are spatially correlated. Moreover, proper estimates of the variability of averages require proper accommodation of spatial correlations in standard error estimates. The analysis of variance procedures in Section 2 accounted for spatial correlations by modeling position and magnet by position interaction effects as random. Similar analyses could be performed on coil-size measurements and any other measurements taken along the length of the magnet. However, the model assumptions for the analysis of variance impose a restriction on the correlation structure, namely that the correlation between two observations is the same for all pairs of positions, the so-called "intraclass" or "equicorrelation" error structure. This may not be a reasonable assumption: the correlation for two adjacent positions may be much larger than for two positions several meters apart.

Cold and warm multipole values were available at each of 24 (nonoverlapping) positions along the lengths of prototype dipole magnets DCA311-319. The two methods that were used to investigate the possible presence of appreciable spatial correlations were: (1) an examination of spatial autocorrelations and (2) an examination of spatial semivariograms.

A.1. Spatial Autocorrelations

The classical approach to analyzing the correlations of temporally or spatially indexed data is through the calculation of the autocorrelations for each of several lags, where a lag is the difference between two index values, in this instance between two positions along the magnet. Denoting a multipole value at position k by m_k and the average across all n positions by $\overline{m}$, the lag d sample autocorrelation is $r(d) = c(d)/c(0)$,

where c(d) represents the sample autocovariance between all multipole values that are d positions apart:

$$c(d) = \sum_{k=1}^{n-d} (m_{k+d} - \overline{m})(m_k - \overline{m}) / (n - d).$$

Figure 6 contains plots of the autocorrelations for the first two cold and warm skew multipoles on DCA311. These plots are typical of plots for the first four skew and normal multipoles on all nine prototype magnets. Since there are only n = 24 positions along the magnets for which both warm and cold multipole values are available, there are a limited number of lags for which sample autocorrelations can be calculated with adequate statistical precision. For the purposes of this illustration, only the first 10 autocorrelations are plotted. Superimposed on the plots are 95% limits (dashed lines). If any of the autocorrelations for lags 1 through 10 exceeds the limits, the autocorrelation is deviating from zero by an amount that cannot be attributed to chance variation; i.e., the sample autocorrelation is significantly different from zero.

In Figure 6 there are two lag-1 autocorrelations that exceed the limits, both on the cold multipoles. This occurs on most of the magnets for all four cold skew multipoles and the warm skew a_2 multipoles. None of the other cold or warm multipoles show consistent significant autocorrelations on the magnets. These plots, therefore, provide evidence of limited spatial autocorrelation, suggesting that it may be possible to ignore spatial autocorrelations for calculating multipole averages across positions on a magnet.

These autocorrelations do not involve the use of warm multipoles to predict cold multipole values in a regression model. One interpretation of these significant autocorrelations is that there are changes in the mean multipole values at different positions. Another is that there is an autoregressive structure to the multipoles. If the former holds, the positional effects of the cold multipoles may be predictable from the warm values. The extent to which the autocorrelations of the cold multipole values are

explained by the warm multipole values can be investigated by a semivariogram analysis of the residuals from a regression fit.

A.2. Sample Semivariograms

Sample semivariograms are measures of spatial variability from which information on spatial correlation can be obtained. For two multipole measurements, provided that the spatial variability is only a function of the distance between two positions and not a function of the position itself, the variogram function is $2\gamma(d) = \mathrm{var}(m_{k+d} - m_k)$. Note that this variogram function assumes "intrinsic" stationarity, a slightly weaker assumption than second-order stationarity commonly assumed for the calculation of autocorrelations. A sample semivariogram is (Cressie 1991, Chapter 2):

$$\hat{\gamma}(d) = \sum_{i=1}^{n(d)} (m_i - m_{i+d})^2 / 2n(d) \ ,$$

where $n(d) = n - d$. Under intrinsic stationarity assumptions, $\hat{\gamma}(d)$ is an unbiased estimator of $\gamma(d)$. If $\hat{\sigma}^2$ denotes the estimated variance of the measurements, spatial covariances can be estimated by $\hat{C}(d) = \hat{\sigma}^2 - \hat{\gamma}(d)$ and the corresponding spatial correlations by $\hat{\rho}(d) = 1 - \hat{\gamma}(d) / \hat{\sigma}^2$ if spatial second-order stationarity can be assumed. A key characteristic of the sample variogram values is that they are constant, apart from sampling error, as a function of the lag d whenever the multipoles are uncorrelated. A substantive increase in the semivariogram values as a function of d, especially for small lags, indicates that the spatial correlations are decreasing as a function of the distance between positions on a magnet.

Semivariogram plots (not included here) of the residuals from least squares fits of the cold to the warm multipole values were examined for each of the nine prototype magnets. Few general comments can be made about the residual semivariogram plots. In some instances, notably the a_2 residual semivariogram plots, the plotted semivariogram values (versus position lag) appeared to be randomly scattered about a horizontal line.

This is the pattern expected if the residuals derive from a model with constant variance and no spatial correlations as a function of position; i.e., a white-noise model. On the other hand, the a_1 residual semivariogram plots sometimes appeared consistent with a white-noise model (e.g., magnets 311, 316, 317, 319) and sometimes exhibited linear (e.g., magnets 312, 313, 315, 318) or cyclic (e.g., magnet 314) trends as a function of position lag.

The trends in the residual semivariogram plots indicate that improved modeling of the position effects would be needed to determine the importance of spatial correlations among the multipole values. The plots of the a_2 residual semivariogram values suggested that the spatial correlations may be small, if they exist. The trends in the plots of the other multipole semivariogram values leaves such a general claim uncertain. It was hoped that the inclusion of coil size, collar, and other physical magnet measurements might account for the remaining position effects. Comprehensive modeling of cold multipole measurements based upon physical magnet measurements and warm multipole values were not conducted prior to the termination of the project; however, two preliminary analyses did show promise and are reported in the next two sections.

B. Azimuthal Coil-Size Measurements

For each of the prototype magnets DCA311, DCA314, and DCA316-319, cold multipole values were modeled as a function of coil-size measurements in a simple linear regression model. The magnets used in this analysis had at least four repeat multipole measurements at each position and are the same ones used in the variance component assessment in Section III. For this analysis, averages of the four repeat measurements were modeled. Since the coil size measurements were regarded as being very precise, with little or no measurement error, no account of measurement error was attempted in this feasibility study.

Coil-size measurements were available at 192 positions along each of the magnets but multipole measurements were taken at only 26 equally spaced positions. The multipole measurements at the two end positions often were inconsistent with those at the other 24 positions. This was expected by the magnet physicists due to curvature effects of the coil windings at the ends of the magnets. The two end positions were not used in the regression analyses. The remaining 24 multipole measurements were matched with coil-size measurements by averaging the eight (nonoverlapping) coil-size measurements closest to each multipole measurement position. The effect of this averaging was that some of the features noticeable in Figure 4 are less noticeable in the averages. The averaging may have cost some in the predictive ability of the model fits, but it was the approach required by the project physics.

Multipole values were fit to an eight-term linear regression model. The eight predictors were the four quadrant coil-size measurements for both the inner and the outer coils. In order to have a realistic appraisal of the ability of the coil-size measurements to predict the multipole values, measurements on five magnets were used to predict the sixth. Figure 7 shows a summary of the results for skew multipole a_1. The solid line segments identify nominal 95% prediction intervals whereas the plotted points are the actual multipole values for the excluded magnet. While there is much room for improvement, these results were encouraging because there were so few magnets available to build the prediction equations. Also, these were prototype magnets, several of which had known imperfections. Moreover, even with the paucity of data, the prediction intervals all were within the rms limit of the target value of the a_1 skew multipole.

C. Cold/Warm Measurements

An issue of great importance for certifying magnet performance was the possible use of room temperature multipole measurements to predict cryogenic values. Just as the cold multipole measurements are subject to a variety of measurement errors, so are the

warm measurements. Figure 2 showed that the magnitude of the measurement errors for cryogenic skew a_1 multipole measurements was very small relative to the variation by position in the average multipole values. Figure 8 is a similar figure for four repeats of warm skew a_1 multipole measurements for magnet DCA311. The warm values are much more variable than the cold values on all the prototype magnets. The size of these measurement errors precludes the use of ordinary least squares prediction equations.

If measurement error variability changes substantially by position, variability estimates would be needed for statistical modeling purposes at each position along the length of the magnet. If this variability is reasonably stable, however, then the modeling of the multipole values is considerably less complicated. Examination of all the repeat data for the prototype magnets revealed the presence of a small number of outliers. These were removed and standard deviation estimates from each position were found to be consistent across magnet positions. These position-by-position standard deviations were then combined to produce estimated measurement error standard deviations for each multipole on each magnet.

Tables 3 and 4 display the estimated standard deviations for each magnet and each multipole. All magnets for which repeats were available are included in the tables, not just those magnets with repeats on both cold and warm multipoles. An important question that arises from an examination of Tables 3 and 4 is whether the standard deviations for each magnet are sufficiently similar that a single standard deviation can be used to represent the variability of a multipole. A cursory examination of the standard deviations in the tables suggests considerable variability across magnets. For the cold multipoles, DCA318 consistently has the smallest standard deviations and DCA316 has the largest. For the warm multipoles, DCA318 again consistently has the smallest standard deviations and DCA311 has the largest (note that there are no standard deviation estimates for warm multipoles on DCA316). The question of whether a common standard deviation could be

used effectively to represent the variability of all the magnets was still unresolved at the termination of the project.

Measurement error modeling (Fuller 1987, Chapter 1) was used to accommodate the measurement errors in the warm multipole measurements. Figure 9 shows the results of this preliminary study for skew multipole a_1. For half of the magnets the measurement error modeling produced magnet mean multipole predictions that were closer to the actual averages than least squares, and vice versa.

V. Concluding Remarks

These analyses of magnet characteristics and magnetic field quality, while incomplete due to the small number of prototype magnets available for inclusion in the studies and to the premature termination of the project, were on the threshold of the development of a comprehensive quality assurance program for particle accelerators. The blending of classical quality control methods with new procedures based on physical magnet measurements, indirect (multipole) measurements of magnetic field quality, and comprehensive statistical modeling would have been critically tested only years after the installation of the first magnets. Successful demonstration of the value of these investigations might have contributed to greater acceptance of statistical quality assurance methods in other important scientific endeavors. While this final test was not accomplished, there is much of value in the knowledge gained from the efforts. The primary lesson learned that can be the focus of future quality assurance efforts is that the combination of less expensive coil dimension measurements and room temperature magnetic field multipole measurements could produce usable predictions of the ultimate cryogenic magnet performance.

Acknowledgments

The authors wish to acknowledge and thank Subir Ghosh for organizing this memorial volume to Donald B. Owen. Special thanks are given to Doug Pollock, who was instrumental in securing our involvement on this project. Technical and computational support of Huchen Fei, Nalin Perera, Ping Li, and Marcia Stoesz, who were graduate students in the Department of Statistical Science during this work, is gratefully acknowledged. Support on this work was provided by the Department of Energy and the Superconducting Super Collider.

References

Cressie, N. (1991). *Statistics for Spatial Data.* New York: John Wiley and Sons, Inc.

Fuller, W.A. (1987). *Measurement Error Models*, New York: John Wiley and Sons, Inc.

List of Tables

Table 1. Multipole Specification Limits.

Table 2. Analysis of Magnet and Position Effects on Skew Multipole a_1.

Table 3. Estimated Cold Magnet Measurement Error Standard Deviations.

Table 4. Estimated Warm Magnet Measurement Error Standard Deviations.

List of Figures

Figure 1. Cutaway Schematic of Proton Beam Tube and Coil Windings for Dipole Magnets.

Figure 2. Repeat Measurements on Skew Multipole a_1.

Figure 3. Ratios of Multipole Standard Deviations to RMS Specifications.

Figure 4. Azimuthal Coil-Size Measurement Deviations.

Figure 5. Opposite Quadrant Azimuthal Coil-Size Measurement Deviations.

Figure 6. Autocorrelations for Cold and Warm Skew Multipoles.

Figure 7. Prediction of a_1 Multipoles from Coil-Size Measurements.

Figure 8. Repeat Measurements on Warm Skew Multipole a_1, Magnet DCA311.

Figure 9. Prediction of Cold a_1 Skew Multipole Averages from Warm a_1 Averages.

Table 1. Multipole Specification Limits.

Multipole	Magnitude ($x10^{-4}$)	rms ($x10^{-4}$)
	Skew Multipoles	
a_1	.04	1.25
a_2	.032	.35
a_3	.026	.32
a_4	.01	.05
	Normal Multipoles	
b_1	.04	1.25
b_2	.80	1.15
b_3	.026	.16
b_4	.08	.22

Table 2. Analysis of Magnet and Position Effects on Skew Multipole a_1.

Source	Degrees of Freedom	Mean Square	Estimated Variance Component	Estimated Standard Deviation
Magnet (M)	5	14.66	.1498	$\hat{\sigma}_m$=.387
Position (P)	23	.36	.0031	$\hat{\sigma}_p$=.056
M x P	115	.28	.0703	$\hat{\sigma}_{mp}$=.265
Error	432	$.47x10^{-4}$	$.47x10^{-4}$	$\hat{\sigma}_e$=.007
Total	575			

Table 3. Estimated Cold Magnet Measurement Error Standard Deviations.

Multipole	DCA 311	DCA 314	DCA 315	DCA 316	DCA 317	DCA 318	DCA 319	DCA 320
a_1	.00534	.00724	.00612	.01143	.00537	.00316	.00570	.00845
a_2	.00179	.00235	.00198	.00275	.00179	.00114	.00203	.00244
a_3	.00202	.00233	.00211	.00356	.00229	.00106	.00225	.00293
a_4	.00124	.00149	.00142	.00200	.00135	.00063	.00171	.00123
b_1	.00471	.00635	.00543	.01017	.00516	.00234	.00532	.00747
b_2	.00176	.00213	.00211	.00238	.00196	.00109	.00211	.00133
b_4	.00124	.00154	.00148	.00153	.00143	.00057	.00152	.00117
b_6	.00050	.00059	.00049	.00079	.00048	.00022	.00053	.00052

Table 4. Estimated Warm Magnet Measurement Error Standard Deviations.

Multipole	DCA311	DCA314	DCA315	DCA318	DCA320
a_1	0.4494	0.4739	0.4225	0.2869	0.3436
a_2	0.1330	0.1006	0.0833	0.0719	0.0782
a_3	0.1470	0.0974	0.0681	0.0386	0.0768
a_4	0.0974	0.0539	0.0426	0.0202	0.0412
b_1	0.4159	0.3214	0.2432	0.2296	0.2340
b_2	0.1150	0.0975	0.0802	0.0686	0.0737
b_4	0.0741	0.0580	0.0433	0.0231	0.0397
b_6	0.0294	0.0279	0.0153	0.0082	0.0154

Fig. 1. Cutaway Schematic of Proton Beam Tube and Coil Windings for Dipole Magnets.

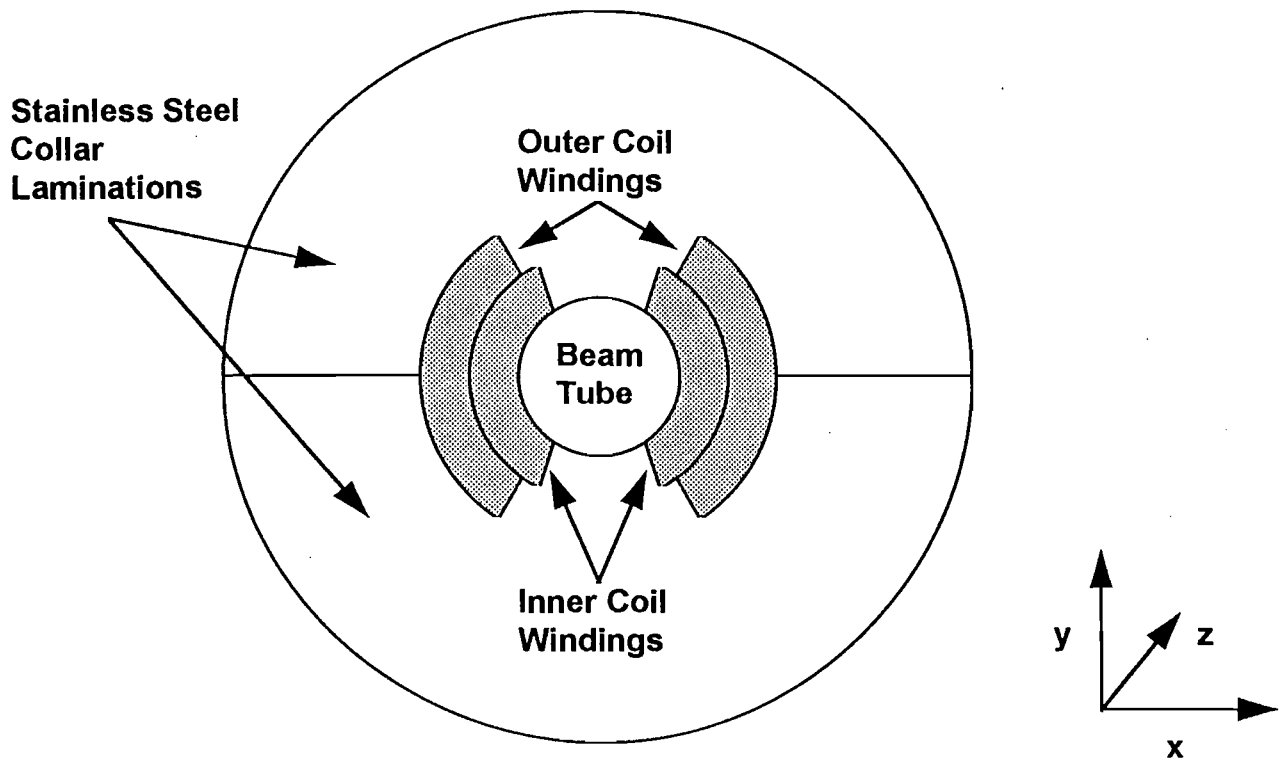

Fig. 2. Repeat Measurements on Skew Multipole a1.

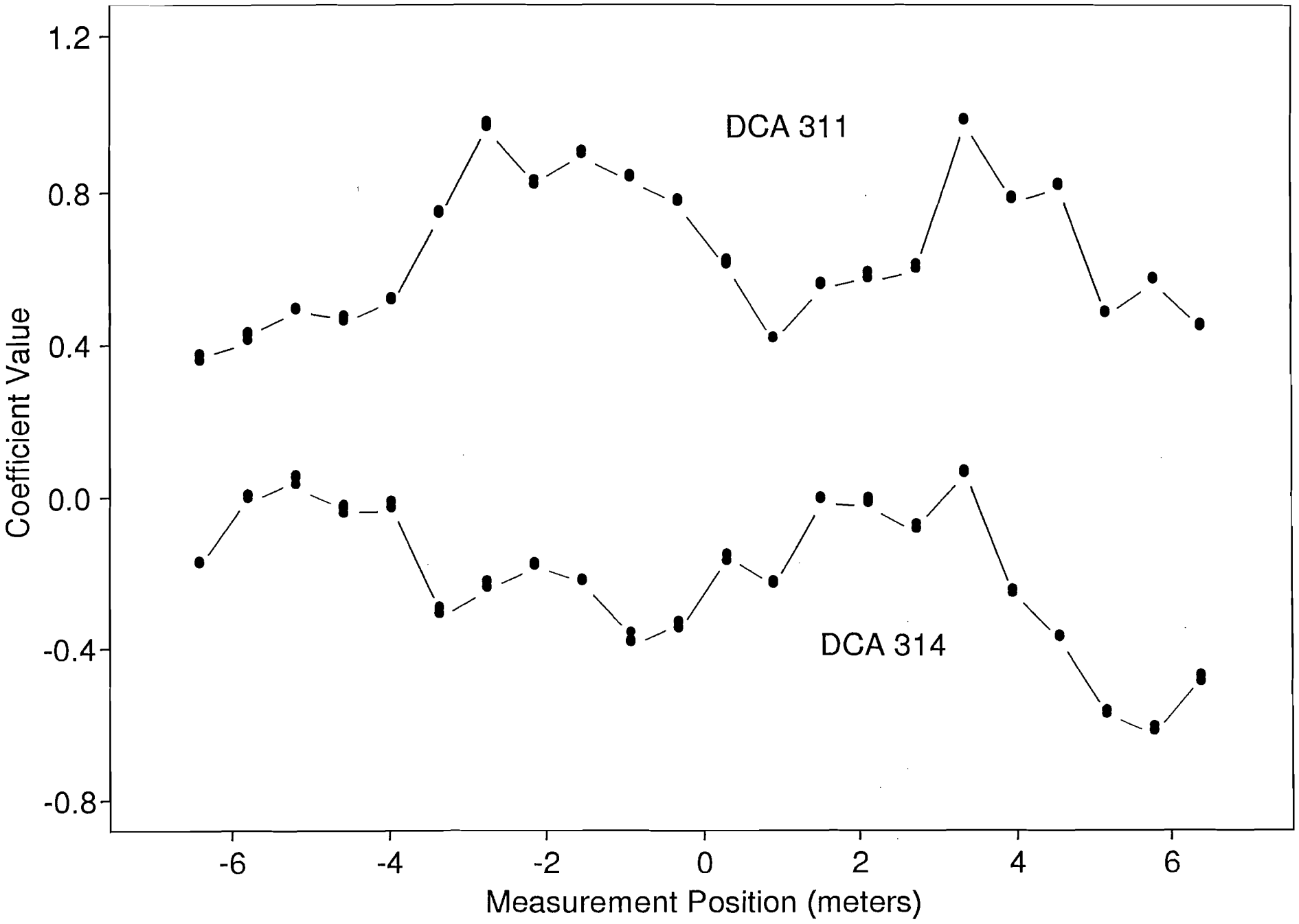

Fig. 3. Ratios of Multipole Standard Deviations to RMS Specifications.

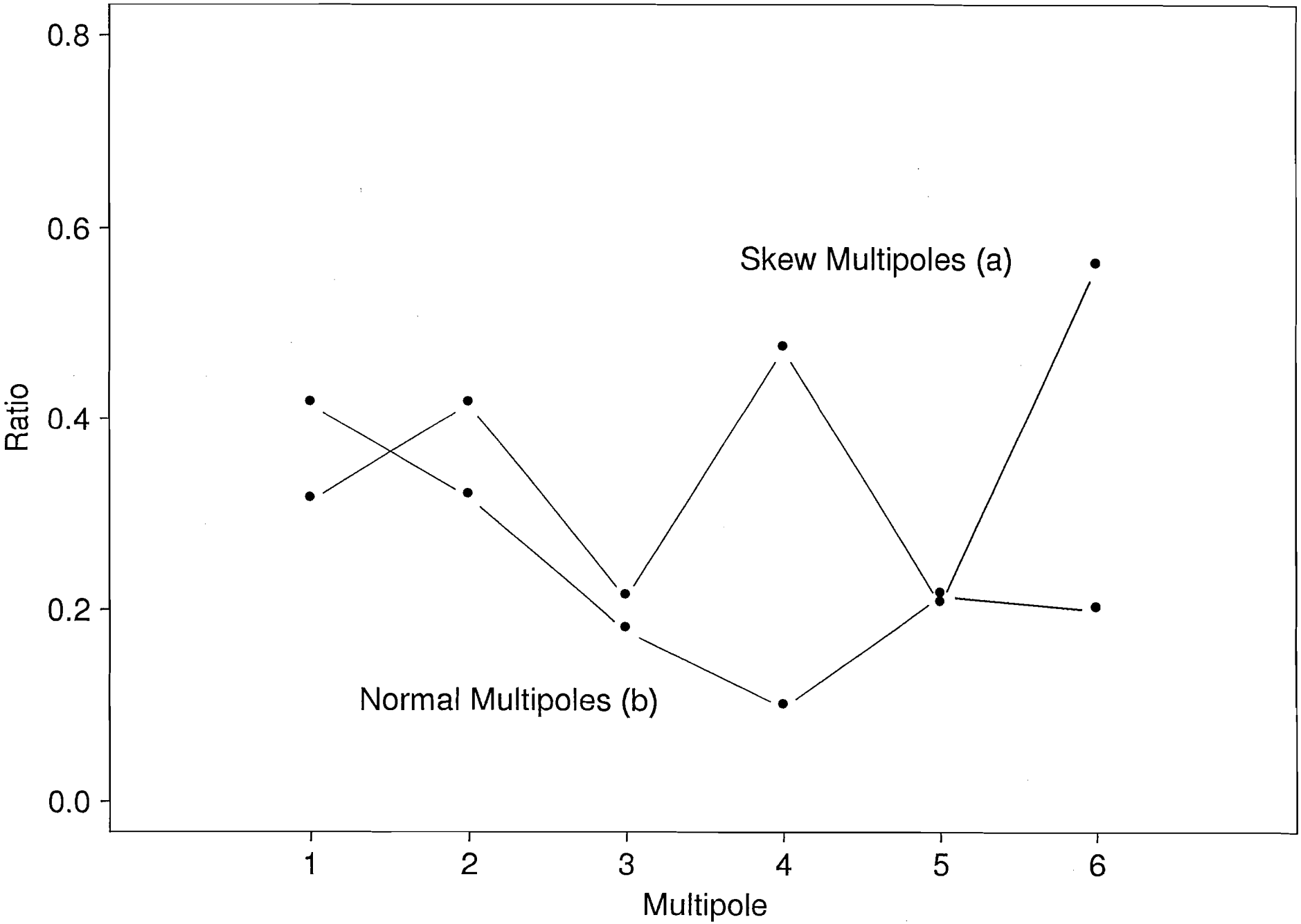

Fig. 4. Azimuthal Coil-Size Measurement Deviations.

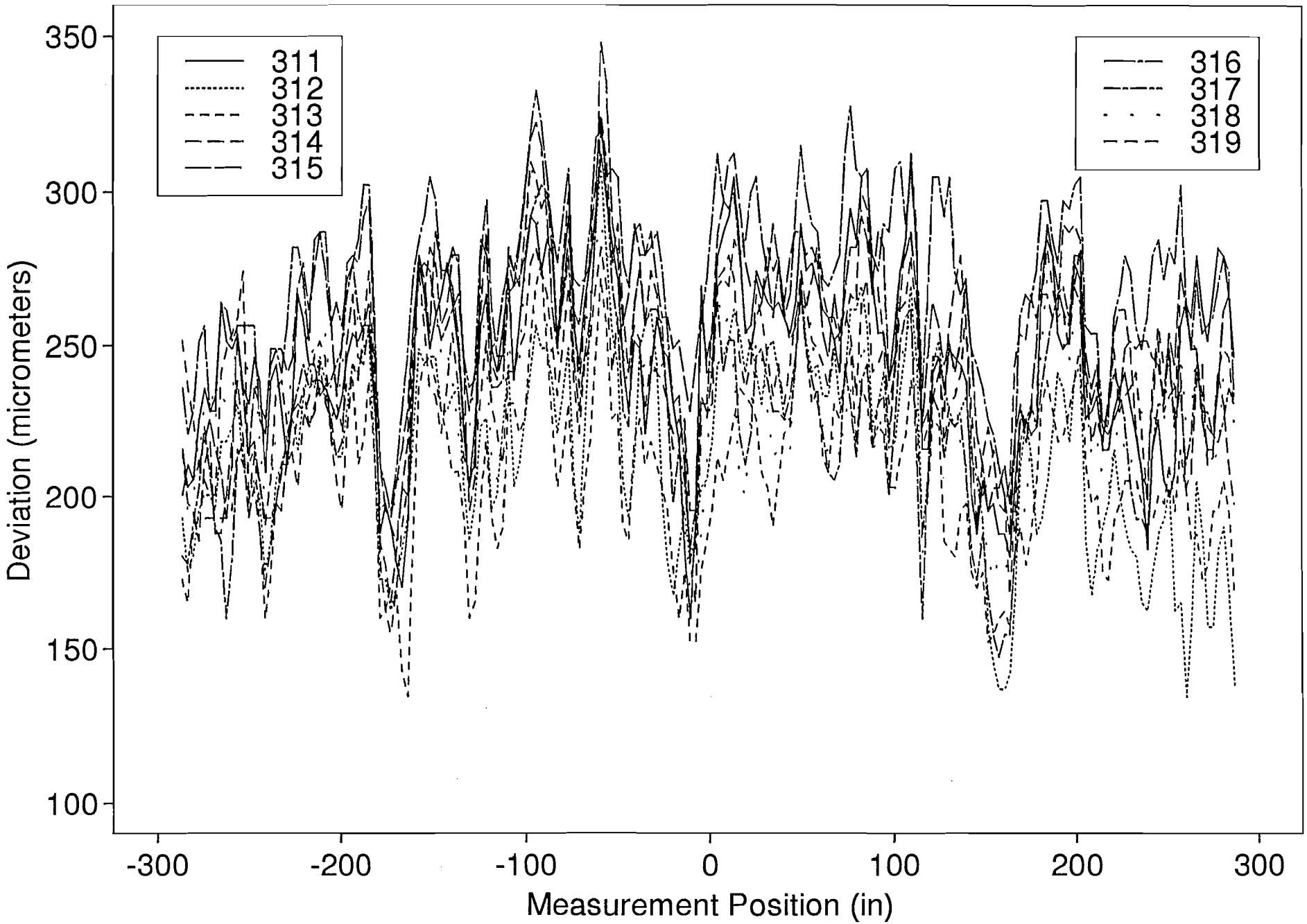

Fig. 5. Opposite Quadrant Azimuthal Coil-Size Measurement Deviations.

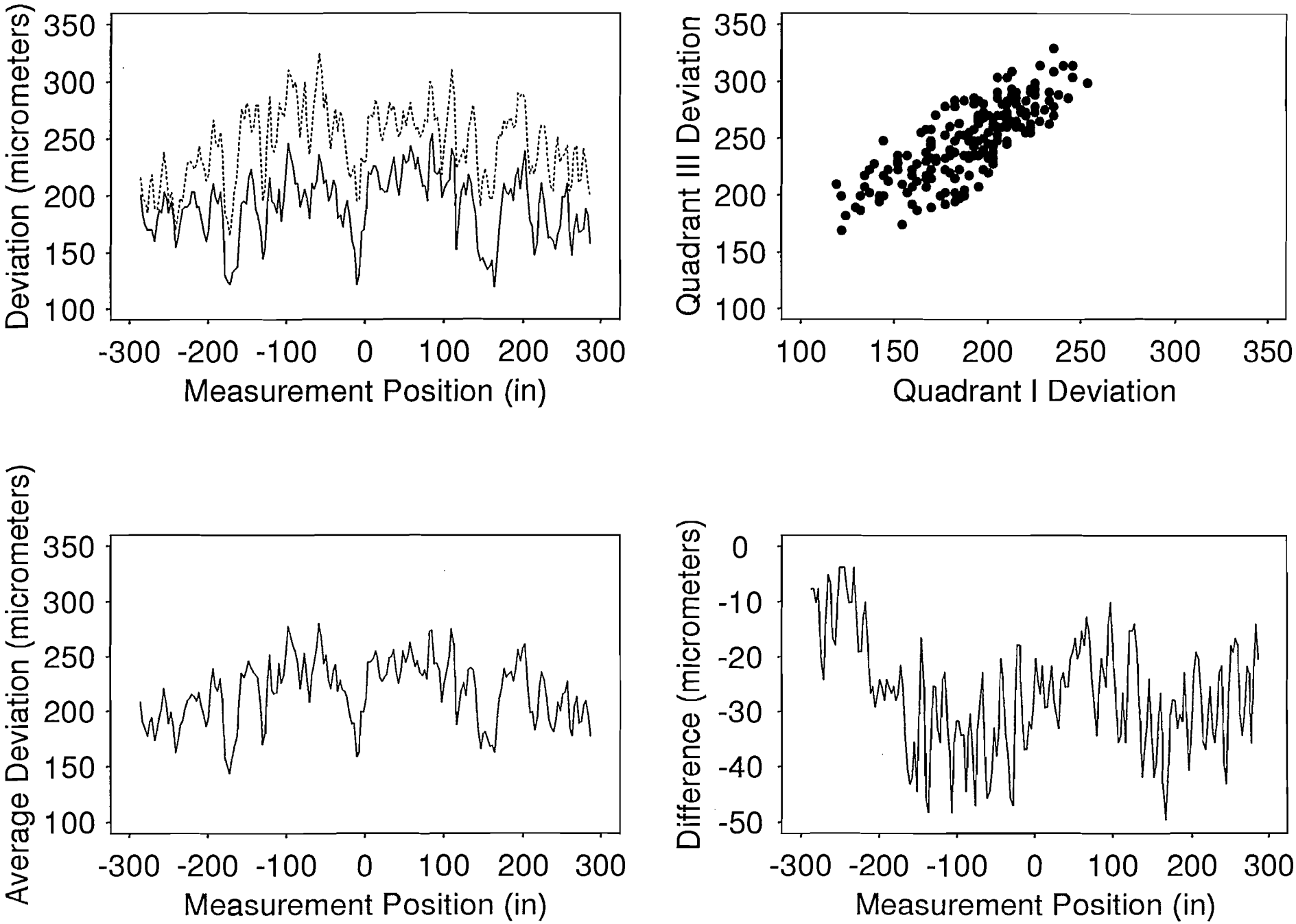

Fig. 6. Autocorrelations for Cold and Warm Skew Multipoles.

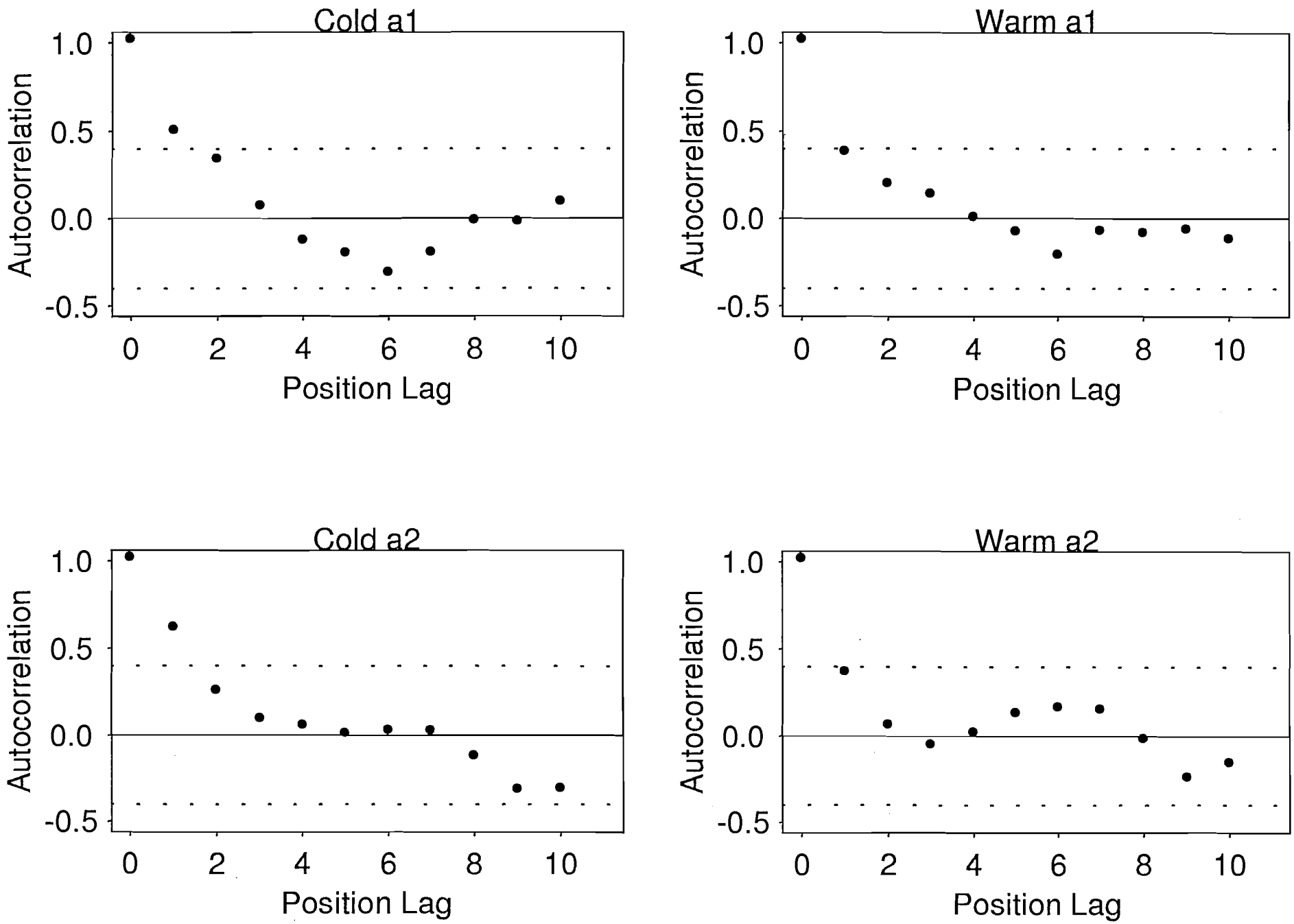

Fig. 7. Prediction of a1 Multipoles from Coil-Size Measurements.

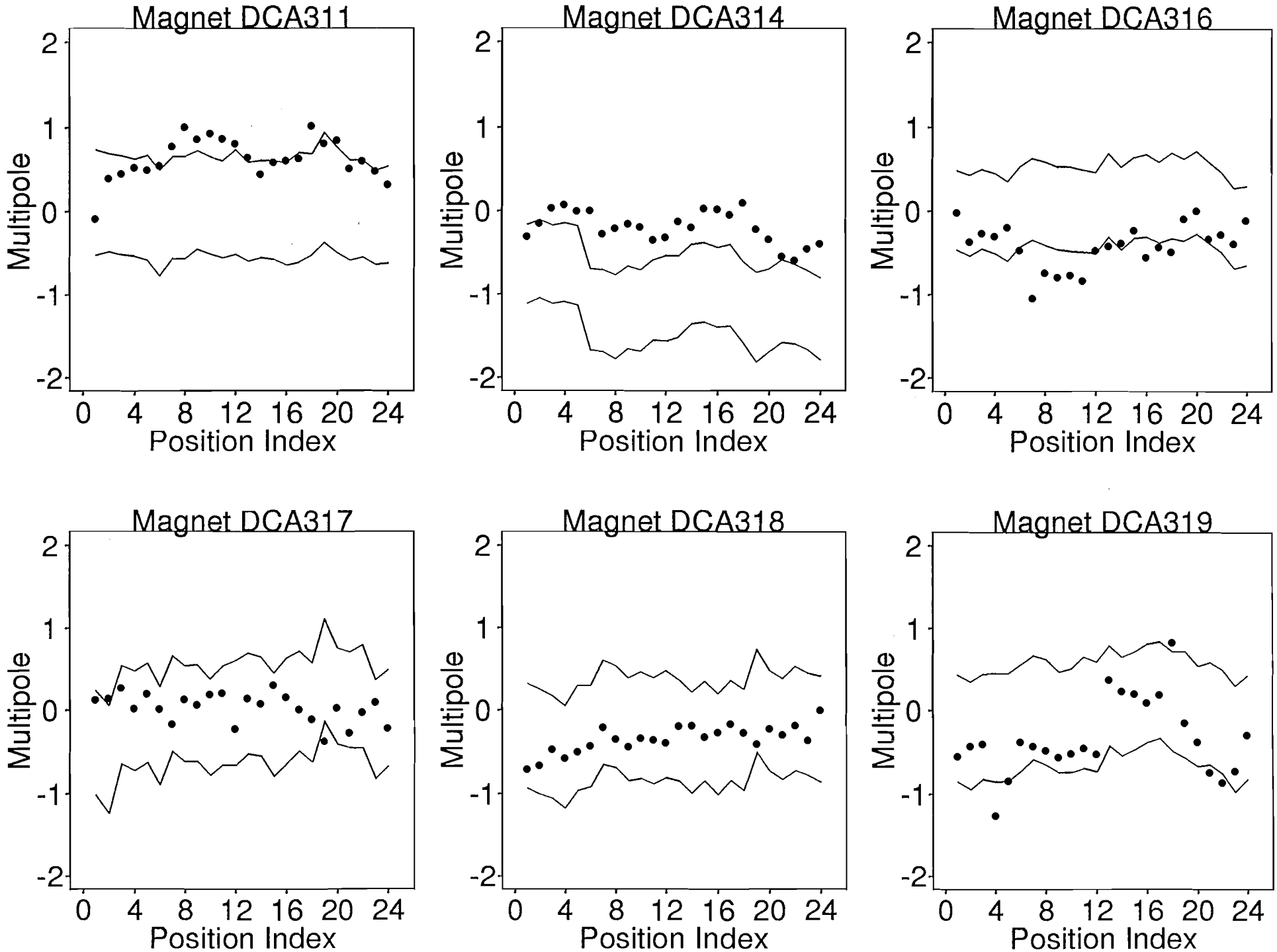

Fig. 8. Repeat Measurements on Warm Skew Multipole a1, Magnet DCA311.

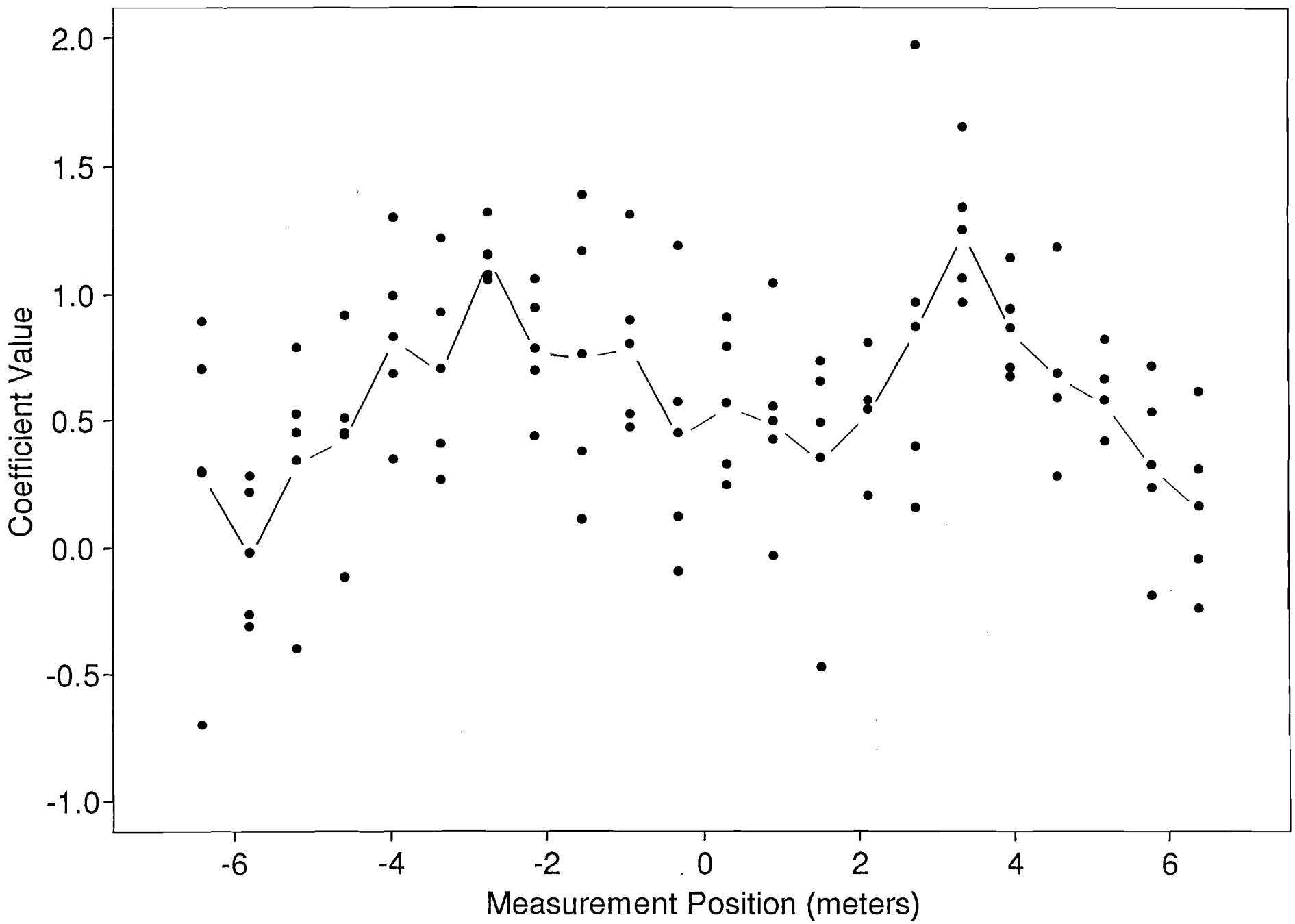

Fig. 9. Prediction of Cold a1 Multipole Averages from Warm a1 Averages.